

## Synchrotron Spectra of Compact VLBI-Jets

A. P. Lobanov

*Max-Planck-Institut für Radioastronomie, Bonn, Germany*

J. A. Zensus<sup>1</sup>

*National Radio Astronomy Observatory, Charlottesville, VA, USA*

**Abstract.** We discuss the feasibility and prospects of broad-band spectral imaging based on quasi-simultaneous multi-frequency VLBI observations.

### 1. Spectral Imaging as a Tool for Probing the VLBI-Jets

Improved quality of VLBI data and increased degree of complexity in recent theoretical (particularly numerical) models of compact parsec-scale jets raise a demand for new approaches to extraction of information from high-resolution images. Measuring the turnover point in the synchrotron emission spectrum appears to be an attractive way to satisfy this demand and probe the physical conditions in VLBI-jets. The turnover frequency  $\nu_m$  can be used as an indicator for velocity gradients produced by an ultra-relativistic plasma channel embedded in jet (Sol, Pelletier, & Asséo 1989) or velocity and pressure gradients due to Kelvin-Helmholtz instabilities (Hardee, Clark, & Howell 1995). Combined with the turnover flux density,  $S_m$ , the turnover frequency also provides an estimate of magnetic field strength in the jet.

### 2. Mapping the Turnover Frequency Distribution

To map the  $\nu_m$  and  $S_m$  distributions in VLBI-jets, we use quasi-simultaneous VLBA observations at 3 or more frequencies. We describe elsewhere (Lobanov 1996) the data reduction procedure applied for making the spatial sensitivities at different frequencies as uniform as possible. In the corresponding spectral index maps, the typical confusion level due to uneven Fourier sampling at individual frequencies is about 5 mJy/beam. This enables confident measurements in fairly extended jet regions, given a sufficiently wide frequency coverage and proper alignment of images at different frequencies. Image alignment is discussed in detail in Lobanov (1996).

For spectral fitting we use the standard synchrotron spectrum  $I(\nu) \propto \nu^{2.5}(1 - \exp[\nu^{\alpha-2.5}])$ . Details of the fitting procedure are given in Lobanov & Zensus (1998). If the fitted  $\nu_m$  lies outside the observing frequency range  $[\nu_l, \nu_h]$ , we apply the local curvature correction, so as to compensate for inadequate frequency coverage. To make the correction, we measure the optically thin spectral index,  $\alpha_{\text{fit}}$ , and local curvature,  $\kappa_{\text{fit}} = (d^2S/d\nu^2)[1 + (dS/d\nu)^2]^{-1/3}$ , of the fitted spectrum within the  $[\nu_l, \nu_h]$  interval. We then compare it with the local curvature of the standard synchrotron spectrum, and derive the correction factor,  $\xi(\alpha_{\text{fit}}, \kappa_{\text{fit}})$ .

---

<sup>1</sup>Present address: Max-Planck-Institut für Radioastronomie, Bonn, Germany.

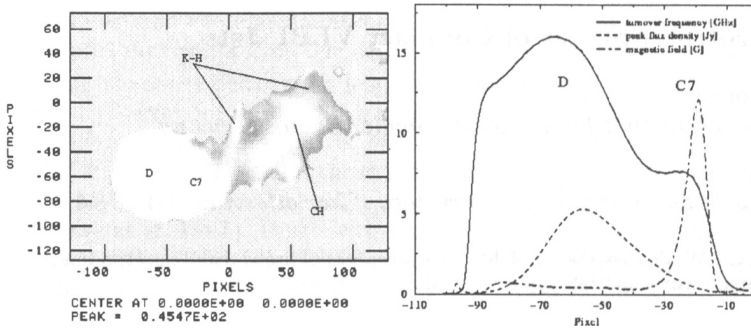


**Figure 1.** Left panel: turnover frequency distribution in 3C 345. The saturation level is  $\nu_m = 10$  GHz, to better represent the extended parts of the source. The restoring beam width is 12 pixels (1.2 mas). The core (D) is centered at pixel  $(-60, -60)$ . C7 is the brightest superluminal feature in the jet at 1995.5. Spectral feature “CH” may result from a channel with ultra-relativistic plasma embedded in the jet. The oblique features “K-H” may reflect the velocity or pressure gradients produced by Kelvin–Helmholtz instabilities. Right panel: turnover frequency (solid), turnover flux density (dashed), and magnetic field (dot-dashed) profiles along the jet ridge line ( $y = -60$ ). The core is at  $x = -60$ .

### 3. Synchrotron Spectrum of 3C 345

Figure 1 (left panel) shows a turnover frequency map of 3C 345 made from VLBA data at 5, 8, 15, and 22 GHz (June 24, 1995). The core region is saturated to better represent the extended jet. Some edge effects due to spurious emission in the individual VLBA maps are seen at  $\approx 3$  mJy level. The bright elongated features seen in the extended jet are possibly the traces of velocity gradients in the perturbed jet plasma (due to an ultra-relativistic plasma or Kelvin–Helmholtz instabilities propagating in the jet). We feel however that the existence of these patterns needs to be verified by new observations.

In the right panel of Figure 1, we show the profiles of  $S_m$ ,  $\nu_m$ , and magnetic field,  $B_j$  along the jet ridge line. We use  $B_{5pc} = 0.4$  G (Lobanov 1996) to calibrate the  $B_j$  values. The  $B_j$  profile in 3C 345 shows a significant increase at the location of the most prominent jet feature (C7, at  $x = -20$ ), while the highest values of both  $S_m$  and  $\nu_m$  are observed in the core. The enhancement of magnetic field seen in C7 is most likely due to the compression by a strong relativistic shock propagating in the jet of 3C 345.

**Acknowledgments.** The National Radio Astronomy Observatory is a facility of the National Science Foundation, operated under a cooperative agreement by Associated Universities, Inc.

### References

- Hardee P. E., Clark D. A., & Howell D. A. 1995. *ApJ*, **441**, 644–664.
- Lobanov, A. P. 1996. *Ph.D. Thesis*, NMIMT, Socorro, USA.
- Lobanov, A. P., & Zensus, J. A. 1998. *ApJ*, submitted.
- Sol H., Pelletier G., & Asséo, E. 1989. *MNRAS*, **237**, 411–429.